Stimulated Brillouin scattering modeling for high-resolution, time-domain distributed sensing

Aldo Minardo[1], Romeo Bernini[2], and Luigi Zeni[1]

[1]*Dipartimento di Ingegneria dell'Informazione – Seconda Università di Napoli*
Via Roma, 29, 81031 Aversa, Italy
aldo.minardo@unina2.it, zeni@unina.it

[2]*Istituto per il Rilevamento Elettromagnetico dell'Ambiente*
Consiglio Nazionale delle Ricerche, Via Diocleziano, 328 – 80124, Naples, Italy
bernini.r@irea.cnr.it;

Abstract: Starting from the standard three-wave SBS coupled equations, we derive a novel expression describing Brillouin interaction between a pulsed pump wave with a finite cw component, and a Stokes continuous wave counter-propagating along a single-mode optical fiber. The derived integral equation relates the time-domain Stokes beam amplification to the Brillouin frequency distribution. The proposed model permits an accurate description of the Brillouin interaction even for arbitrarily-shaped pump pulses, and can be efficiently employed for improving the accuracy and the resolution of SBS-based distributed sensors. The validity and the limits of the proposed model are numerically analyzed and discussed.

OCIS codes: (290.5900) Scattering, stimulated Brillouin; (060.2370) Fiber optics sensors; (060.4370) Nonlinear optics, fibers

References and links

1. T. Horiguchi, K. Shimizu, T. Kurashima, and Y. Koyamada, "Advances in distributed sensing techniques using Brillouin scattering," Proc.SPIE **2507**, 126-135 (1995).
2. X. Bao, A. Brown, M. DeMerchant, and J. Smith, "Characterization of the Brillouin-loss spectrum of single-mode fibers by use of very short (< 10-ns) pulses," Opt. Lett. **24**, 510-512 (1999), http://www.opticsinfobase.org/abstract.cfm?URI=ol-24-8-510
3. V. Lecoeuche, D. J. Webb, C. N. Pannell, and D. A. Jackson, "Transient response in high-resolution Brillouin-based distributed sensing using probe pulses shorter than the acoustic relaxation time ," Opt. Lett. **25**, 156-158 (2000), http://www.opticsinfobase.org/abstract.cfm?URI=ol-25-3-156
4. X. Bao, Q. Yu, V. P. Kalosha, and L. Chen, "Influence of transient phonon relaxation on the Brillouin loss spectrum of nanosecond pulses," Opt. Lett. **31**, 888-890 (2006), http://www.opticsinfobase.org/abstract.cfm?URI=ol-31-7-888
5. Y. Wan, S. Afshar V., L. Zou, L. Chen, and X. Bao, "Subpeaks in the Brillouin loss spectra of distributed fiber-optic sensors," Opt. Lett. **30**, 1099-1101 (2005), http://www.opticsinfobase.org/abstract.cfm?URI=ol-30-10-1099
6. R. Bernini, A. Minardo, and L. Zeni, "An accurate high-resolution technique for distributed sensing based on frequency-domain Brillouin scattering," Photon. Technol. Lett. **18**, 280-282 (2006).
7. S. -B. Cho, J. -J. Lee, and I. -B. Kwon, "Strain event detection using a double-pulse technique of a Brillouin scattering-based distributed optical fiber sensor," Opt. Express **12**, 4339-4346 (2004), http://www.opticsinfobase.org/abstract.cfm?URI=oe-12-18-4339
8. K. Kishida, C.-H Lee, and K. Nishiguchi, "Pulse pre-pump method for cm-order spatial resolution of BOTDA," Proc. SPIE **5855**, 559-562 (2005).
9. A. W. Brown, B. G. Colpitts, and K. Brown, "Distributed sensor based on dark-pulse Brillouin scattering," Photon. Technol. Lett. **17**, 1501-1503, (2005).
10. G. P. Agrawal, *Nonlinear Fiber Optics* (Academic, San Diego, Calif., 1995).
11. R. J. LeVeque, "Wave propagation method algorithms for multi-dimensional hyperbolic systems," J. Comp. Phys. **131**, 327-353 (1997).
12. A. Minardo R. Bernini, L. Zeni, L. Thevenaz, F. Briffod, "A reconstruction technique for long-range stimulated Brillouin Scattering distributed fiber-optic sensors: experimental results," Meas. Sci. Technol., **16**, 900-908, (2005).

#80368 - $15.00 USD Received 22 Feb 2007; revised 18 Jun 2007; accepted 25 Jun 2007; published 2 Aug 2007

13. X. Bao, J. Dhliwayo, N. Heron, D. J. Webb, and D. A. Jackson, "Experimental and theoretical studies on a distributed temperature sensor based on Brillouin scattering," J. Lightwave Technol. 13, 1340-1348, (1995).
14. E. Licthman, R. G. Waarts, and A. A. Friesem, "Stimulated Brillouin scattering excited by a modulated pump wave in single-mode fibers," J. Lightwave Technol. **7**, 171-174 (1989).

1. Introduction

Stimulated Brillouin scattering (SBS) is one of the most dominant nonlinear effects in single-mode optical fibers. It consists in the coupling between two counter-propagating optical waves, the pump and the Stokes wave, and an acoustic wave. Interaction reaches its maximum for a precise value of the frequency shift between the two optical waves, which depends on the temperature and strain conditions in the material.

Distributed sensing in an optical fiber is commonly obtained by use of a cw beam and a counter-propagating pulsed beam. One measures the intensity of the transmitted cw beam as a function of the frequency shift to resolve the Brillouin gain spectrum. Positional information is obtained through a time-domain analysis; shorter pulses increase the spatial resolution. However, Brillouin profile is broadened to a Gaussian-like profile as the pulse width decreases below the phonon lifetime, thus reducing the accuracy of temperature/strain measurements [1]. On the other hand, the use of a pulsed pump beam with a small cw component (base) results in a spectral narrowing, arising from the background acoustic intensity generated by interaction between the cw beam and the baseline of the pulsed beam [2-3]. Experimentally, one can control the baseline level by adjusting the bias voltage of the electro-optic modulator used for pulse forming. Although such a spectral narrowing is desirable to perform accurate temperature/strain estimations, it has been also reported that such a base for the pulsed beam may result in distortions in Brillouin gain curves, leading to errors in the determination of the Brillouin frequency, especially when one is trying to measure local fiber conditions that are close to the average condition in the whole fiber [3-4]. Furthermore, the presence of subpeaks in the Brillouin spectrum originating from off-resonance relaxation oscillations in the Brillouin time-domain [5], can lead to misinterpretation due to the difficulty to distinguish these subpeaks from the peaks due to strain–temperature variations along the fiber.

The above considerations suggest the opportunity to develop an accurate time-domain model to be employed in a reconstruction algorithm, which would allow corrections of the recorded spectra and thus a more-precise estimation of the fiber condition [3, 6]. Such an algorithm would require the generation of synthetic Brillouin signals corresponding to a particular fiber condition. Although this is feasible in principle by numerically integrating the three coupled-wave equations governing SBS interaction, this approach would lead to unacceptable computation times.

In this letter, we show that, under some hypotheses that are valid in many practical cases, an integral expression relating the Brillouin signal to the gain distribution along the fiber can be formulated. Such expression can be numerically evaluated in an efficient way, opening the possibility to implement iterative reconstruction algorithms. The derived expression is also of interest, because it allows us to gain a better physical insight into the phenomena involved in high-resolution Brillouin measurements. On the other hand, the proposed model can be employed not only to describe the SBS interaction in standard Brillouin optical time-domain analysis (BOTDA) configurations, but, more generally, it can be applied to analyze the SBS interaction between a launched cw beam and a counter-propagating pump beam with an arbitrary waveform. Hence, the model is also of interest for studying recently proposed measurement schemes, involving e.g. the use of a double-pulse [7], a pulse pre-pump [8], or a dark pulse [9].

#80368 - $15.00 USD Received 22 Feb 2007; revised 18 Jun 2007; accepted 25 Jun 2007; published 2 Aug 2007

2. Theoretical description

The method followed to derive our model is based on approaching the SBS equations in the frequency domain. Such an approach has the advantage that it leads to a more easy-to-handle solution with respect to methods directly working in the time domain. We start from the following three-wave SBS transient model [10], where the linear optical attenuation of the fiber has been neglected:

$$\left(\frac{\partial}{\partial z}+\frac{n}{c}\frac{\partial}{\partial t}\right)E_p = -QE_s, \tag{1a}$$

$$\left(-\frac{\partial}{\partial z}+\frac{n}{c}\frac{\partial}{\partial t}\right)E_s = Q^* E_p, \tag{1b}$$

$$\left(\frac{\partial}{\partial t}+\Gamma\right)Q = \frac{1}{2}\Gamma_1 g_B E_p E_s{}^* \tag{1c}$$

where E_p, E_s, and Q are the amplitudes of the pulsed pump, the cw Stokes, and the acoustic fields, respectively; g_B is the SBS gain coefficient; *c* is the light velocity in the vacuum, *n* is the linear refractive index of the fiber; $\Gamma = \Gamma_1 + j\Delta$, where $\Gamma_1 = 1/(2\tau)$ (τ = 10 ns is the phonon lifetime for silica fibers) is the damping rate and $\Delta(z) = \omega_{pp} - \omega_B(z)$ is the *z*-dependent detuning frequency, i.e. the difference between the pump-probe frequency shift and the local Brillouin frequency.

The boundary conditions for Eqs. (1) are $E_S(L,t) = E_{sL}$, and $E_P(0,t) = E_{P0}(t)$, where $E_{P0}(t)$ represents the pump waveform at the input section. When considering a pulsed pump beam, a continuous spectrum for the pump, Stokes and acoustic fields must be considered.

The slowing-varying amplitudes can be written as:

$$E_P(z,t) = \int_{-\infty}^{+\infty} \mathbf{E_P}(z,\omega')\exp\left[j\omega'\left(t-\frac{n}{c}z\right)\right]d\omega' \tag{2}$$

$$E_S(z,t) = \int_{-\infty}^{+\infty} \mathbf{E_S}(z,\omega'')\exp\left[j\omega''\left(t+\frac{n}{c}z\right)\right]d\omega'' \tag{3}$$

$$Q(z,t) = \int_{-\infty}^{+\infty} \mathbf{Q}(z,\Omega)\exp\left[j\Omega\left(t-\frac{z}{v_a}\right)\right]d\Omega \tag{4}$$

In Eqs. (2-4), the symbols ω', ω'' and Ω represent the angular frequency of the pump field amplitude, the angular frequency of the Stokes field amplitude, and the angular frequency of the acoustic field amplitude, respectively. By substituting Eqs. (2-4) in Eq. (1c), and solving for the generated acoustic wave, the following equation for the Stokes wave amplitude can be derived in the frequency domain:

$$\frac{\partial}{\partial z}\mathbf{E_s}(z,\omega) = -\frac{g_B\Gamma_1}{2}\int_{\omega''}\mathbf{E_p}(z,\omega'')\exp\left(-2j\frac{n}{c}\omega''z\right) \times\left[\int_{\omega'}\frac{\mathbf{E_p^*}(z,\omega')\mathbf{E_s}(z,\omega'-\omega''+\omega)}{\Gamma_1 - j(\Delta(z)+\omega''-\omega)}\cdot\exp\left(2j\frac{n}{c}\omega' z\right)d\omega'\right]d\omega'' \tag{5}$$

#80368 - $15.00 USD Received 22 Feb 2007; revised 18 Jun 2007; accepted 25 Jun 2007; published 2 Aug 2007

Details on the analytical derivation of Eq. (5) can be found in Appendix. The physical meaning of Eq. (5) is the following: The integral in the square brackets represents the acoustic wave component at frequency ω''-ω, which interacts with the pump spectral component at frequency ω'', giving rise to a Stokes signal at frequency ω. Integration of Eq. (5) is difficult due to the inter-coupling between the different components of the Stokes spectrum. The problem can be greatly simplified if we consider that the Stokes intensity is cw at the input section (z = L), while it acquires more spectral components during the propagation along the fiber due to SBS. For pump pulse widths comparable to or shorter than the phonon lifetime, the Stokes modulated signal is typically two or three orders of magnitude below the cw component. Hence, we can safely assume that only the cw component of the Stokes beam contributes significantly to acoustic wave generation by interaction with the pump spectrum, i.e., the spectrum of the acoustic wave is similar to that of the pump field. From a mathematical point of view, this is equivalent to assume a Dirac Delta function for the Stokes field in the square brackets of Eq. (5). Hence, the convolution integral over ω' is reduced to the only term for which ω'=ω''-ω. Equation (5) is then simplified as:

$$\frac{\partial}{\partial z}\mathbf{E_s}(z,\omega) = -\frac{g_B\Gamma_1}{2}\int_{\omega''}\frac{\mathbf{E_p}(z,\omega'')\mathbf{E_p^*}(z,\omega''-\omega)E_s^{CW}(z)}{\Gamma_1 - j(\Delta(z)+\omega''-\omega)}\exp\left(-2j\frac{n}{c}\omega z\right)d\omega'' \quad (6)$$

where $E_s^{CW}(z)$ represents the stationary Stokes field along the fiber. The above equation indicates that each component of the acoustic wave spectrum at frequency ω''-ω interacts with the pump spectral component at frequency ω'', contributing to the overall Stokes spectral component at frequency ω. Equation (6) can be integrated along z, provided that the pump spectrum is known for each section along the fiber. For not excessively long fibers, we can apply the undepleted pump approximation. Under this hypothesis, together with the boundary condition $\mathbf{E_s}(L,\omega)=0$, we get the final solution to the Stokes amplitude at $z = 0$:

$$\mathbf{E_s}(0,\omega) = \mathbf{E_s}(0,\omega) - \mathbf{E_s}(L,\omega) = \frac{g_B\Gamma_1}{2}\int_0^L G(z,\omega)\exp\left(-2j\frac{n}{c}\omega z\right)dz \quad (7)$$

where L is the fiber length and:

$$G(z,\omega) = E_s^{CW}(z)\int_{\omega'}\frac{\mathbf{E_p}(0,\omega')\mathbf{E_p^*}(0,\omega'-\omega)}{\Gamma_1 - j(\Delta+\omega'-\omega)}d\omega' \quad (8)$$

Note that for a Hermitian pump spectrum, the above integral can be written as a convolution integral:

$$G(z,\omega) = E_s^{CW}(z)\cdot\left(\mathbf{E_p}(0,\omega)\otimes\frac{\mathbf{E_p}(0,\omega)}{\Gamma_1 - j(\Delta(z)+\omega)}\right) \quad (9)$$

In Eqs. (7-9), $\mathbf{E_p}(0,\omega)$ is the pump spectrum at the launch (z = 0) section and $\mathbf{E_s}(0,\omega)$ is the spectrum of the transmitted (z = 0) Stokes signal. The convolution in Eq. (9) means that any pair of pump spectrum frequencies differing by ω contributes to the frequency ω of the transmitted Stokes spectrum. The latter can be inverse-Fourier-transformed, in order to achieve the time-domain Stokes field at z = 0. Finally, the transmitted Stokes power can be calculated as $P_s(0,t) = |E_s(0,t)|^2 / A_{eff}$, where A_{eff} is the effective area of the fiber. Note that the integral in Eq. (8) can be safely restricted to the range of frequencies over which $\mathbf{E_p}(\omega)$ is

#80368 - $15.00 USD Received 22 Feb 2007; revised 18 Jun 2007; accepted 25 Jun 2007; published 2 Aug 2007

significantly higher than zero. Instead, the Brillouin gain $G(z,\omega)$ (and consequently the Stokes spectrum) may extend to higher frequencies: Actually, the ω'-component of the pump spectrum may give a contribution to higher frequencies ($\omega>\omega'$) of the Stokes spectrum. We underline that, although the model has been developed by supposing amplification of the cw beam at the expense of the pulsed beam, the model can be equally applied in the case of a pulsed Stokes beam, where loss is induced on a cw pump beam. In such a case, it is sufficient to invert the roles of the pump and Stokes beams, while a negative SBS gain coefficient g_B should be considered. Furthermore, Eqs. (7-9) can be evaluated not only for a pump beam consisting of a single pulse (with or without a baseline), but in general for an arbitrary pump spectrum. Hence, the model can be applied in order to analyze the characteristics of the SBS spectrum when using any specific pump waveform, or, conversely, to determine the optimal pulse waveform to be employed in order to achieve a desired SBS spectrum.

3. Numerical results

The validity of the model described by Eq. (7) has been tested by comparing, for a number of test-cases, the Stokes signal calculated by the proposed model, with the fields calculated by directly solving Eq.s (1). The latter were solved by the LeVeque wave propagation method [11], based on the time updating of the initial solution resulting from the SBS stationary equations. Unless otherwise specified, numerical tests were performed for an input pump power of 10 mW, an input Stokes power of 1 mW, and a Brillouin gain $g_B/A_{eff} = 0.2$.

The first numerical test was performed on a uniform 10-m-long fiber. The time instant when the pulse enters the fiber was set to 8 ns, whereas the pulse width and rise/fall times were set to 10 ns and 0.1 ns, respectively. The Stokes spectrum was calculated for a frequency interval ranging from 0 to 1 GHz, with a step of 3 MHz. The quantity plotted in Fig. 1 refers to the difference between the output Stokes power at $z = 0$ and the input Stokes power at $z = L$, calculated for different detuning frequencies and extinction ratios (ER). The latter is defined as the ratio between the maximum pump power and the minimum (cw) pump power. Comparison of the time-domain waveforms demonstrates the accuracy of the proposed method. The normalized norm difference between the signals never exceeded 6 ‰. Note that the computation time needed to solve Eqs. (1) and Eq. (7) is very different: For this example, the time required to solve Eqs. (1) for a single detuning frequency and extinction ratio was about 30 minutes on a Pentium 4 processor with a 3.60-GHz clock frequency, running under MATLAB environment, whereas solving Eq. (7) on the same platform took about 12 seconds (including the time required to calculate the stationary solution).

The next test was performed for the same pulse condition, but on a fiber length of 50 m, with a 1-meter-long 30 MHz-large perturbation in the middle of the fiber. Stokes spectrum was calculated up to 1 GHz with a frequency step of 600 kHz, while the extinction ratio was set to 20 dB. Figure 2 clearly indicates that our model is successful in determining the Brillouin time-domain signals. In particular, the inset shows the accuracy of the model in describing the prolonged Brillouin gain at $\Delta = 30$ MHz, due to the fact that, even after the pulse passes the perturbation, the phonon (acoustic) field at $\Delta = 30$ MHz is still sustained by the interaction of the pulse cw level and Stokes signals [4]. On the other hand, for this longer fiber, we also note that pump depletion induces an error in our model increasing with distance, especially for zero detuning, reaching a maximum deviation of about 7 ‰ at the pulse exit location. Maximum norm deviation from the solution of Eqs. (1) is about 3 % in this case. Therefore, for fiber lengths of tens of meters or more, the approximation of undepleted pump used in our model may give rise to an error increasing with the distance from the pulse launch section. Obviously, for a fixed fiber length, such an error will decrease for weaker input Stokes powers. We also underline that a given error in Stokes signal modeling does not imply necessarily an equivalent error in Brillouin frequency determination when employing iterative reconstruction algorithms. For instance, we experimentally showed in Ref. [12] that the error in Brillouin frequency determination due to pump depletion becomes significant for fiber lengths of several km.

#80368 - $15.00 USD Received 22 Feb 2007; revised 18 Jun 2007; accepted 25 Jun 2007; published 2 Aug 2007

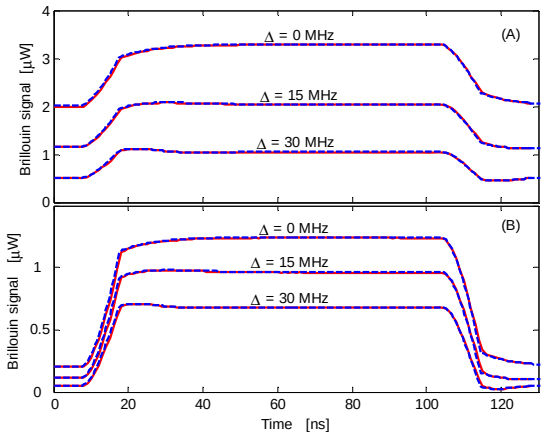

Fig. 1. Stokes amplification time-domain waveforms, as calculated by solving the full model of Eqs. (1) (dashed blue lines) and the model of Eq. (7) (solid red lines). Solutions are calculated for L = 10 m, τ_P = 10 ns, and ER = 10 dB (A) ER = 20 dB (B).

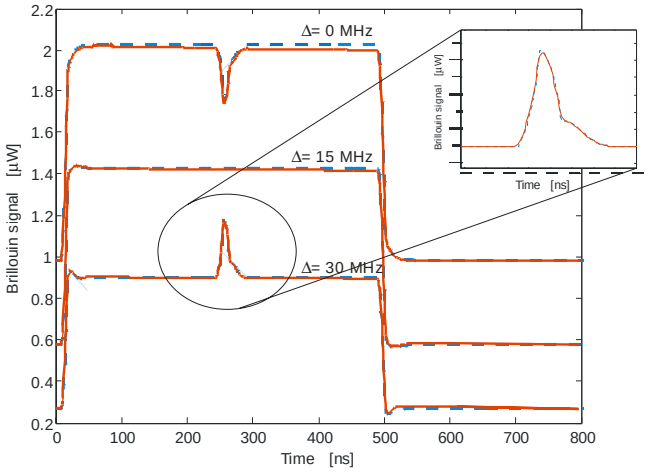

Fig. 2. Stokes amplification time-domain waveforms, as calculated by solving the full model of Eq.s (1) (dashed blue lines) and the model of Eq. (7) (solid red lines). The inset shows a zoom-in view of the perturbed region, at Δ = 30 MHz. Solutions are calculated for L = 50 m, τ_P = 10 ns, and ER = 20 dB.

A successive test was performed on a shorter uniform fiber (L = 1 m) and for a shorter pulse width (τ_P = 1.5 ns). This fiber length was chosen in order to put in evidence the transient effects related to the acoustic wave off-resonance relaxation. Time-domain waveforms were calculated for a detuning frequency ranging from -500 to 500 MHz, with a 10 MHz step. Stokes spectrum was calculated up to 10 GHz, with a frequency step of 10 MHz. Figure 3 shows the Brillouin gain spectrum calculated by using the two methods, at the instant t = 18 ns, i.e. at the instant in which the pulse exits the fiber. Still, we can observe a close agreement between the two calculations (norm difference over the whole frequency range ≈ 1 %). Note the presence of subpeaks in the Brillouin spectrum, originating from off-resonance relaxation oscillations in Brillouin time-domain signals [5].

#80368 - $15.00 USD Received 22 Feb 2007; revised 18 Jun 2007; accepted 25 Jun 2007; published 2 Aug 2007

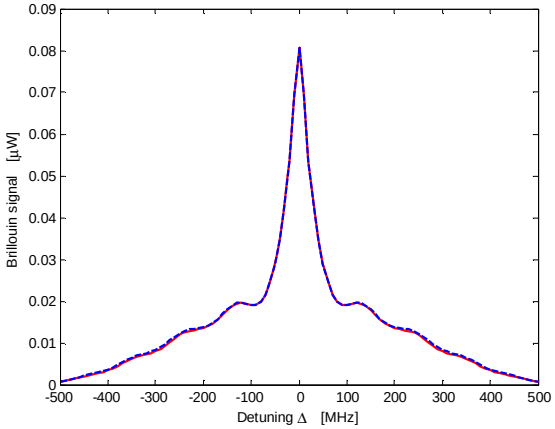

Fig. 3. Brillouin gain spectrum calculated at t = 18 ns, for a uniform 1-meter-long fiber, τ_p = 1.5 ns, ER = 20 dB, by solving the full model of Eqs. (1) (dashed blue line) and the model of Eq. (7) (solid red line).

As a further demonstration of the capability of our method, we performed another test on a 1-meter-long fiber, and for a 1.5-ns-long pulse. However, in this case the fiber was subjected to two 15cm-long, 30 MHz-large perturbations, separated by an unperturbed 15-cm-long central region. The simulation parameters were identical to the ones employed for the latter test. Figure 4 shows the Brillouin gain spectra calculated according to the two methods, in correspondence of three fiber positions, chosen within the first perturbation, the central unperturbed region, and the second perturbation, respectively. It can be seen that the agreement is very good, as both methods display the superposition of two Brillouin gain peaks at each considered section.

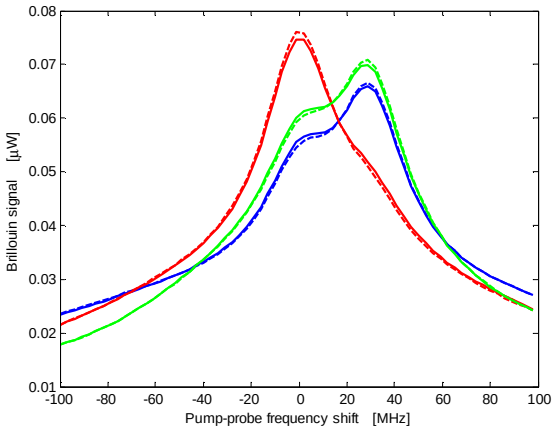

Fig. 4. Brillouin gain spectrum calculated at t = 12.1 ns (blue line), t = 13.6 ns (red line) and t = 15 ns (green line), for a perturbed 1-meter-long fiber, τ_p = 1.5 ns, ER = 20 dB, by solving the full model of Eqs. (1) (dashed lines) and the model of Eq. (7) (solid lines).

Finally, the following analysis was devoted to understand the limits of validity of the proposed model. As discussed earlier, the undepleted pump approximation introduces an error which can be considered negligible for relatively short fibers (let us say $L \leq 10$ m), whereas for longer fibers this error may become significant. In the latter case, a better estimation of

#80368 - $15.00 USD Received 22 Feb 2007; revised 18 Jun 2007; accepted 25 Jun 2007; published 2 Aug 2007

Brillouin signals may be achieved by taking into account the interaction of the pump pulse peak with the cw (dominant) component of the Stokes wave and using the computed pump power distribution into the calculation of Eq. (6). Obviously, the model complexity will increase as well. To demonstrate this possibility, we calculated again the Stokes signal for the 50-meter-long fiber case previously shown in Fig. 2, but considering pump depletion. Results are shown in Fig. 5, where a better agreement between the approximated and exact computations can be noted. In particular, the norm error in this case is about 4 ‰, whereas maximum deviation is about $4 \cdot 10^{-4}$.

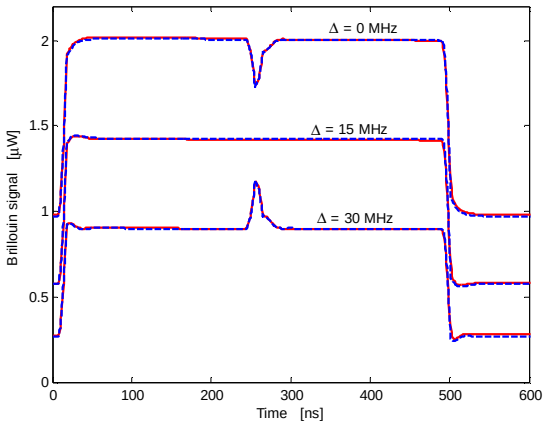

Fig. 5. Stokes amplification time-domain waveforms, as calculated by solving the full model of Eq.s (1) (dashed blue lines) and the model of Eq. (6), in which pump depletion is taken into account (solid red lines). Solutions are calculated for L = 50 m, τ_P = 10 ns, and ER = 20 dB.

On the other hand, we must also consider the error introduced in our model for neglecting the modulated Stokes signal in the calculation of the generated acoustic wave. We can argue that the above assumption is valid as long as the modulated Stokes signal is significantly smaller than the cw counterpart. Under undepleted pump approximation, the maximum modulated Stokes signal can be estimated as: $P_{sL}\left[\exp(g_B / A_{eff} \cdot P_p \cdot W) - 1\right]$, where W is the pump-Stokes interaction length ($W = 1/2\,\tau_p c/n$) and P_{SL} is the input (at z = L) cw Stokes power. Here, we are mainly interested in pulse widths comparable or shorter than the phonon lifetime. Actually, for longer pulse widths, a quasi-stationary model, much simpler than the one expressed by Eq. (7), can be safely employed [13]. By setting a pulse width of 10 ns and an input Stokes power of 1 mW, and imposing a modulated Stokes signal ten times smaller than the input cw component (i.e., 100 μW), we estimate a maximum input pump power of ~ 0.5 W. This means that, for the conditions considered in our example and input pump powers sufficiently smaller than 0.5 W, we may expect that our model will be able to accurately determine the Brillouin signals. To confirm this prevision, we performed a number of simulations for a uniform 10-meters-long fiber, an input Stokes power of 1 mW, and for increasing input pump powers in the range 10 mW - 1 W. Results of this simulation are summarized in Table 1, where we report the normalized norm difference between the two models. Note that the error increases faster when input pump power exceeds 0.5 W. As mentioned earlier, this has to be attributed to the high modulated Stokes signal occurring for these pump levels. Actually, maximum Stokes amplification as calculated by our model for an input pump power of 1 W (not shown here), is about 2.6 % smaller than the one calculated with the full model. This depends on the fact that, neglecting the modulated Stokes signal contribution to the generated acoustic wave, results in an underestimation of the acoustic wave intensity, and consequently of the modulated Stokes signal itself. On the other hand, we

#80368 - $15.00 USD Received 22 Feb 2007; revised 18 Jun 2007; accepted 25 Jun 2007; published 2 Aug 2007

must also underline that such high pump powers are unusual in Brillouin-based measurements, in order to avoid the onset of other nonlinear effects (Raman scattering, self-phase modulation, etc.).

Table 1. Normalized norm difference between the Brillouin signals calculated by solving Eq. (7) and the Brillouin signals calculated by solving Eqs. (1). Solutions are calculated for L = 10 m, τ_P = 10 ns, ER = 20 dB, and input Stokes power = 1 mW.

Total input pump power	10 mW	100 mW	500 mW	1 W
Norm Difference	5.7 ‰	8.4 ‰	9.6 ‰	2.8 %

4. Conclusions

In summary, an analytical expression relating the time-domain Stokes amplification to the Brillouin frequency shift distribution along a single-mode optical fiber has been derived. To the best of our knowledge, this is the first time an analytical expression is derived for the case of a pulsed pump beam, in which the transient effects due to the acoustic wave are (at least partially) taken into account. We underline that the expression given in Ref. [14] for a modulated pump wave is only valid for very long (L > 1 km) fibers.

The derived expression may be employed for fast generation of synthetic Brillouin signals in BOTDA configurations, for each assigned Brillouin frequency shift profile. More generally, the model can be employed to describe SBS interaction between a CW beam and a counter-propagating, arbitrarily-shaped, pulse beam. The accuracy of the proposed model has been evaluated for several numerical test-cases. The results show that the model is accurate enough to be employed in iterative reconstruction algorithms for precise temperature/strain sensing, similarly to previous works published by the Authors [6, 12].

Appendix

We report in this section the analytical derivation of Eq. (5), starting from the SBS coupled-wave equations and the assumptions of Eqs. (2-4).

Substitution of Eqs. (2-4) in Eq. (1c), leads to the following equation:

$$\left(\frac{\partial}{\partial t}+\Gamma\right)Q=\int_{-\infty}^{+\infty}\mathbf{Q}(z,\Omega)(\Gamma+j\Omega)\exp\left[j\Omega\left(t-\frac{z}{v_a}\right)\right]d\Omega$$
$$=\frac{1}{2}\Gamma_1 g_B\int_{-\infty}^{+\infty}\int_{-\infty}^{+\infty}\mathbf{E_P}(z,\omega')\mathbf{E_S^*}(z,\omega'')\exp[j(\omega'-\omega'')t]\exp\left[-j(\omega'+\omega'')\frac{n}{c}z\right]d\omega' d\omega'' \quad (10)$$

By imposing the phase matching conditions, i.e. $\Omega=(\omega'-\omega'')$ and $\Omega/v_a=(\omega'+\omega'')n/c$, Eq. (10) can be rewritten as:

$$\int_{-\infty}^{+\infty}\mathbf{Q}(z,\Omega)(\Gamma+j\Omega)\exp\left[j\Omega\left(t-\frac{z}{v_a}\right)\right]d\Omega$$
$$=\frac{1}{2}\Gamma_1 g_B\int_{-\infty}^{+\infty}\int_{-\infty}^{+\infty}\mathbf{E_P}(z,\omega')\mathbf{E_S^*}(z,\omega'-\Omega)\exp\left[j\Omega\left(t-\frac{z}{v_a}\right)\right]d\Omega\, d\omega' \quad (11)$$

From Eq. (11) we derive:

$$\mathbf{Q}(z,\Omega)=\frac{1}{2}\Gamma_1 g_B\int_{-\infty}^{+\infty}\frac{\mathbf{E_P}(z,\omega')\mathbf{E_S^*}(z,\omega'-\Omega)}{(\Gamma+j\Omega)}d\omega' \quad (12)$$

#80368 - $15.00 USD Received 22 Feb 2007; revised 18 Jun 2007; accepted 25 Jun 2007; published 2 Aug 2007

which can be substituted in Eq. (4), so as to achieve the solution for the acoustic wave:

$$Q(z,t)=\frac{1}{2}\Gamma_1 g_B \int_{-\infty}^{+\infty}\int_{-\infty}^{+\infty}\frac{\mathbf{E_P}(z,\omega')\mathbf{E_S^*}(z,\omega'')}{\Gamma+j(\omega'-\omega'')}\exp[j(\omega'-\omega'')t]\exp\left[-j(\omega'+\omega'')\frac{n}{c}z\right]d\omega'\,d\omega'' \tag{13}$$

By using Eq. (13) and Eqs. (2-3) we can write:

$$-Q^*E_P=-\frac{1}{2}\Gamma_1 g_B\int_{-\infty}^{+\infty}\int_{-\infty}^{+\infty}\int_{-\infty}^{+\infty}\frac{\mathbf{E_P^*}(z,\omega')\mathbf{E_S}(z,\omega'')\mathbf{E_P}(z,\omega''')}{\Gamma^*-j(\omega'-\omega'')}\times\exp[-j(\omega'-\omega''-\omega''')t]\exp\left[j(\omega'+\omega''-\omega''')\frac{n}{c}z\right]d\omega'd\omega''d\omega''' \tag{14}$$

as well as:

$$\left(\frac{\partial}{\partial z}-\frac{n}{c}\frac{\partial}{\partial t}\right)E_S=\left(\frac{\partial}{\partial z}-\frac{n}{c}\frac{\partial}{\partial t}\right)\int_{-\infty}^{+\infty}\mathbf{E_S}(z,\overline{\omega})\exp\left[j\overline{\omega}\left(t+\frac{n}{c}z\right)\right]d\overline{\omega}=\int_{-\infty}^{+\infty}\frac{d\mathbf{E_S}(z,\overline{\omega})}{dz}\exp\left[j\overline{\omega}\left(t+\frac{n}{c}z\right)\right]d\overline{\omega} \tag{15}$$

By equating Eq. (14) and Eq. (15) we achieve:

$$\int_{-\infty}^{+\infty}\frac{\partial\mathbf{E_S}(z,\overline{\omega})}{\partial z}\exp\left[j\overline{\omega}\left(t+\frac{n}{c}z\right)\right]d\overline{\omega}=-\frac{1}{2}\Gamma_1 g_B\int_{-\infty}^{+\infty}\int_{-\infty}^{+\infty}\int_{-\infty}^{+\infty}\frac{\mathbf{E_P^*}(z,\omega')\mathbf{E_S}(z,\omega'')\mathbf{E_P}(z,\omega''')}{\Gamma^*-j(\omega'-\omega'')}\exp[-j(\omega'-\omega''-\omega''')t]\times\exp\left[j(\omega'+\omega''-\omega''')\frac{n}{c}z\right]d\omega'\,d\omega''d\omega''' \tag{16}$$

By imposing $\overline{\omega}=-(\omega'-\omega''-\omega''')$, Eq. (16) can be rewritten as:

$$\int_{-\infty}^{+\infty}\frac{\partial\mathbf{E_S}(z,\overline{\omega})}{\partial z}\exp\left[j\overline{\omega}\left(t+\frac{n}{c}z\right)\right]d\overline{\omega}=-\frac{1}{2}\Gamma_1 g_B\int_{-\infty}^{+\infty}\int_{-\infty}^{+\infty}\int_{-\infty}^{+\infty}\frac{\mathbf{E_P^*}(z,\omega')\mathbf{E_S}(z,\omega'')\mathbf{E_P}(z,\omega'-\omega''+\overline{\omega})}{\Gamma^*-j(\omega'-\omega'')}\exp[j\overline{\omega}t]\times\exp\left[j(2\omega''-\overline{\omega})\frac{n}{c}z\right]d\omega'd\omega''\,d\overline{\omega} \tag{17}$$

From Eq. (17) we achieve:

$$\frac{\partial\mathbf{E_S}(z,\overline{\omega})}{\partial z}=-\frac{g_B\Gamma_1}{2}\int_{-\infty}^{+\infty}\int_{-\infty}^{+\infty}\frac{\mathbf{E_P^*}(z,\omega')\mathbf{E_S}(z,\omega'')\mathbf{E_P}(z,\omega'-\omega''+\overline{\omega})}{\Gamma^*-j(\omega'-\omega'')}\exp\left[j(2\omega''-2\overline{\omega})\frac{n}{c}z\right]d\omega'd\omega'' \tag{18}$$

#80368 - $15.00 USD Received 22 Feb 2007; revised 18 Jun 2007; accepted 25 Jun 2007; published 2 Aug 2007

which, upon a proper change of variables, coincides with the expression of Eq. (5).

As a final remark, if the optical attenuation is not negligible, it is easy to show that Eq. (5) can be generalized as follow:

$$\frac{\partial}{\partial z}\mathbf{E_s}(z,\omega) = -\frac{g_B\Gamma_1}{2}\int_{\omega''}\frac{\mathbf{E_p}(z,\omega'')\mathbf{E_p}^*(z,\omega''-\omega)E_s^{CW}(z)}{\Gamma_1 - j(\Delta(z)+\omega''-\omega)}\exp\left(-2j\frac{n}{c}\omega z\right)d\omega'' + \frac{\alpha}{2}\mathbf{E_s}(z,\omega) \tag{19}$$

where α is the linear optical attenuation along the fiber. Consequently, by following the same procedure described previously, Eq. (7) can be rewritten as:

$$\mathbf{E_s}(0,\omega) = \frac{g_B\Gamma_1}{2}\int_0^L G(z,\omega)\exp\left(-2j\frac{n}{c}\omega z - \alpha\right)dz \tag{20}$$

Acknowledgments

This work was supported by MIUR: PRIN No 2005091408 and COST 299 – FIDES. The Authors gratefully acknowledge Dr. Giuseppe Alì for his help in analytical computations.

#80368 - $15.00 USD Received 22 Feb 2007; revised 18 Jun 2007; accepted 25 Jun 2007; published 2 Aug 2007